Electronic Supplementary Material (ESI) for RSC Advances

Radical cations of end-capped tetrathienoacenes and their π-dimerization controlled by the nature of α-substituents and counterion concentration

Nur S. Rizalman,[a] Cristina Capel Ferrón,[b] Weijun Niu,[c] Arthur L. Wallace,[c] Mingqian He,[c] Russell Balster,[a] John Lampkin,[a] Víctor Hernández,*[b] Juan T. López Navarrete,*[b] M. Carmen Ruiz Delgado,*[b] František Hartl*[a]

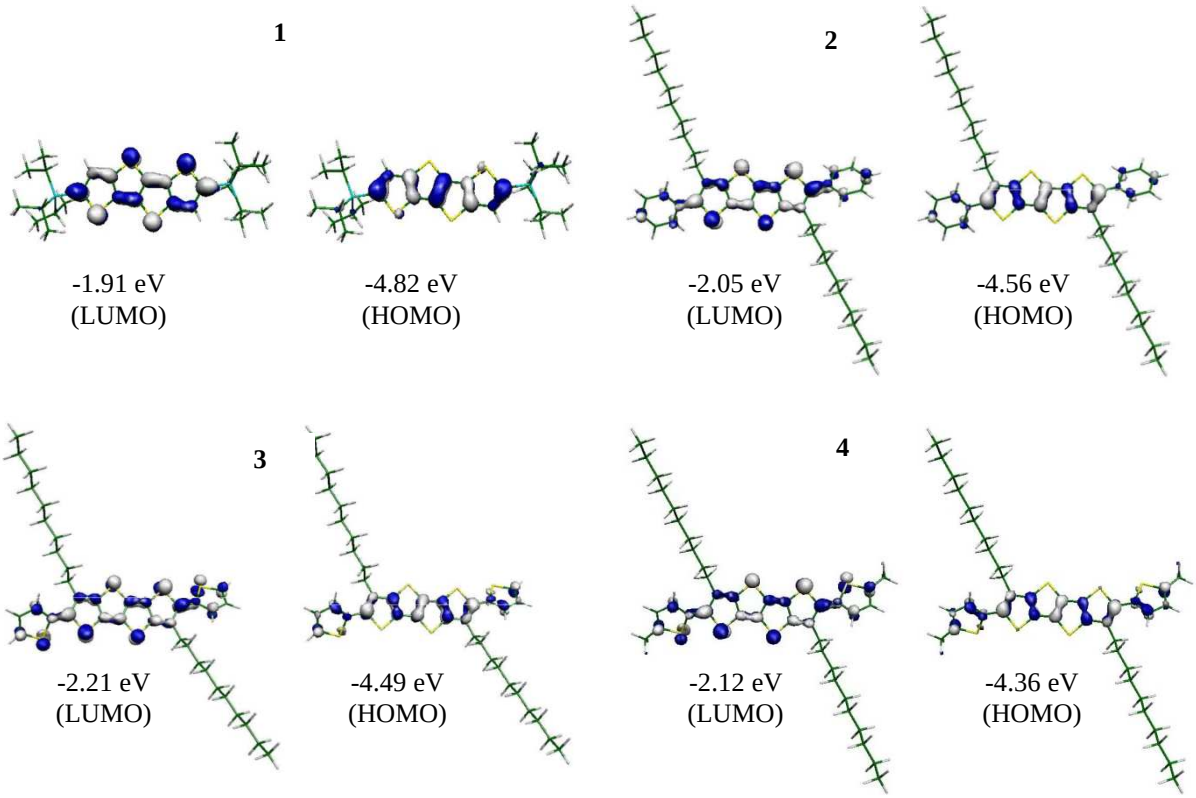

Fig. S1 The molecular orbital topologies and energies of the frontier molecular orbitals of compounds **1-4** computed at the DFT//M06L/6-31G* level.

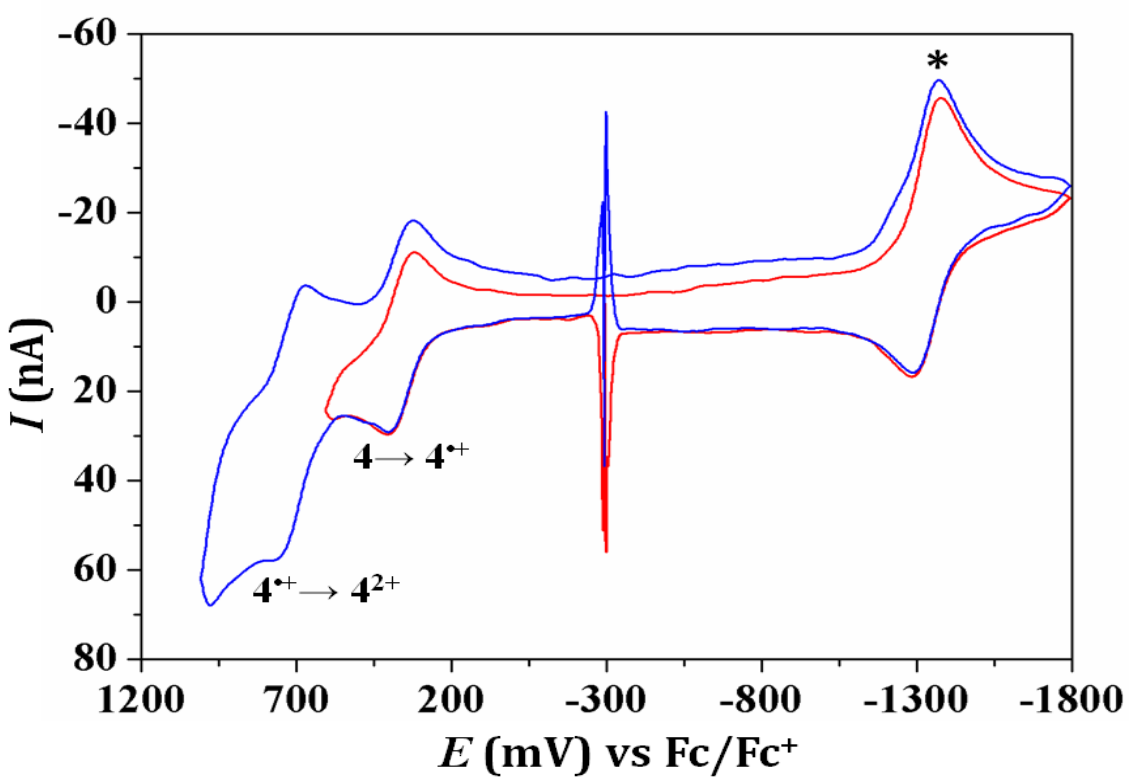

Fig. S2 The cyclic voltammogram of 1.90×10^{-4} M **4** in $CH_2Cl_2/10^{-1}$ M Bu_4NPF_6 at 293 K, using a 128- m platinum microelectrode at the scan rate of 1.2 V s^{-1};

The asterisk denotes the internal standard, cobaltocenium hexafluorophosphate; $E_{½}(Cc/Cc^{+}) = -1.33$ V vs Fc/Fc^{+}.

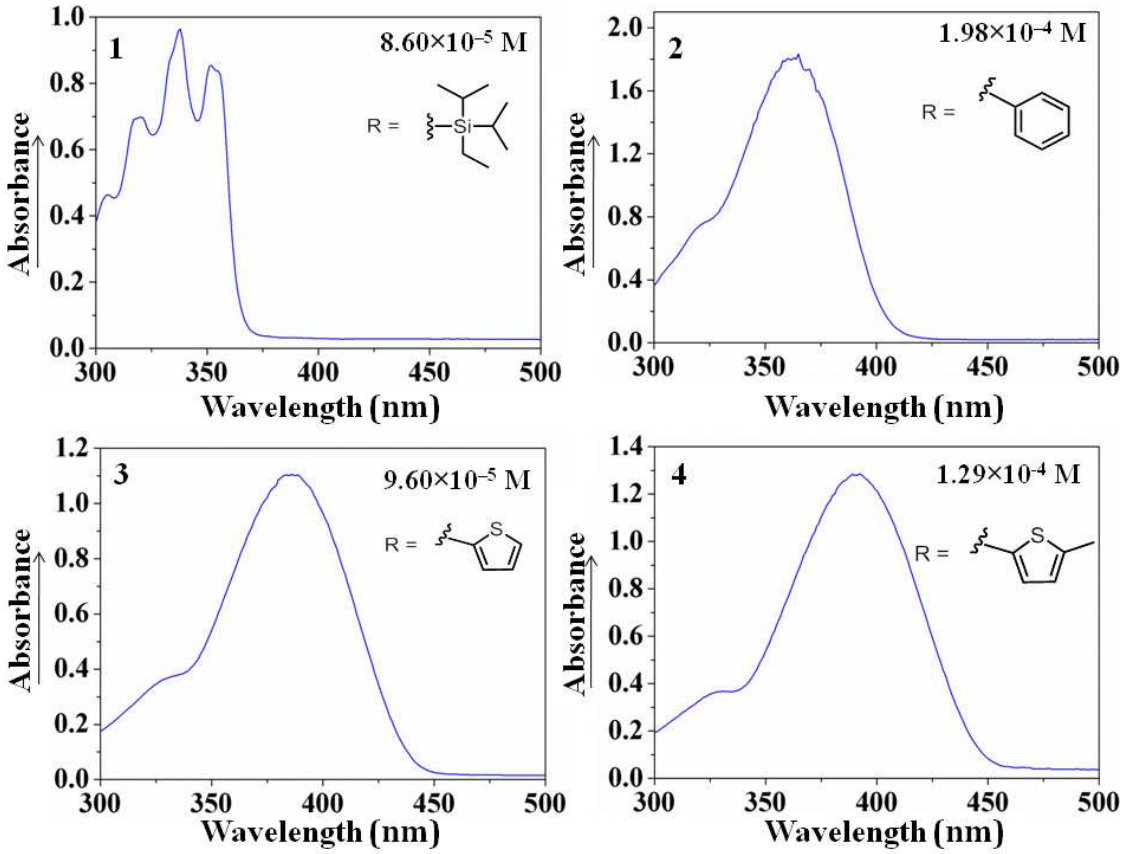

Fig. S3 Electronic absorption spectra of **1-4** (R = α-substituents) in dry argon-saturated dichloromethane, showing the absorption band attributed to the HOMO→LUMO (π→π*) transition according TD-DFT calculations (see Table S1).

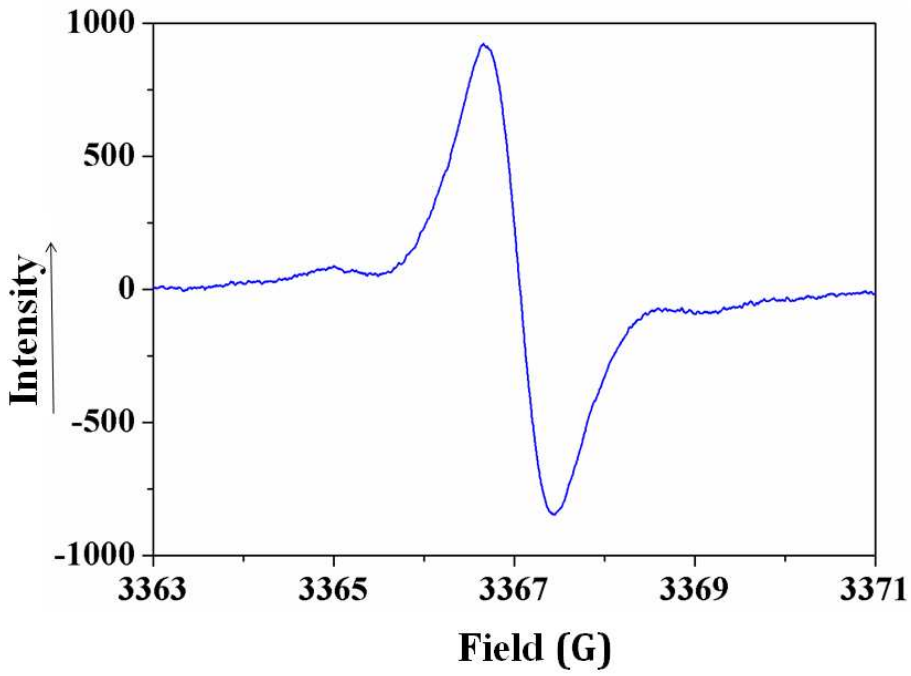

Fig. S4 EPR spectrum of $\mathbf{1}^{\bullet+}$ (g = 2.0014) recorded after the chemical oxidation of 6.6×10^{-5} M **1** with 1 equiv. $TAPF_6$ in dry dichloromethane at 293 K. The spectrum displays ^{29}Si satellites that are also seen in the EPR spectrum of the pentathienoacene analog reported in the literature.[1,2]

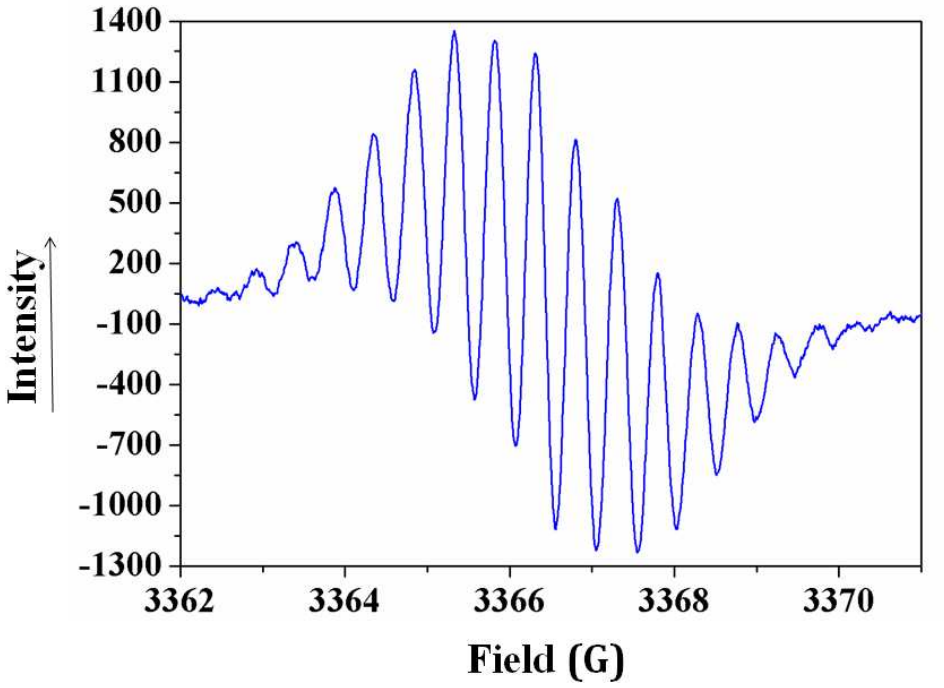

Fig. S5 EPR spectrum of $\mathbf{2}^{\bullet+}$ (g = 2.0018) recorded after the chemical oxidation of 3.6×10^{-5} M **1** with 1 equiv. $TAPF_6$ in dry dichloromethane at 293 K.

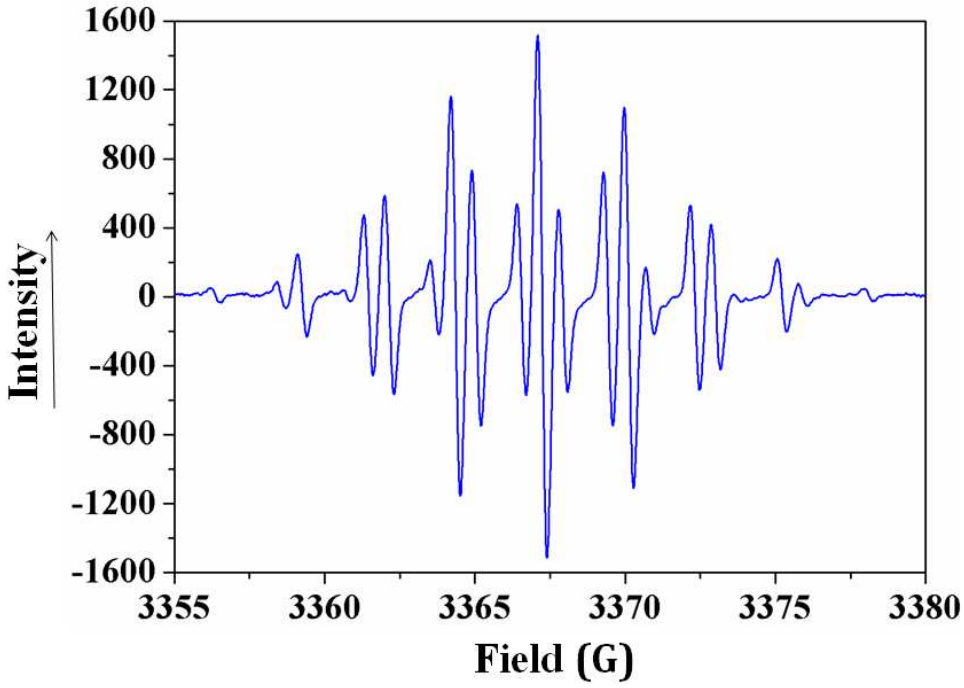

Fig. S6 EPR spectrum of $\mathbf{4}^{\bullet+}$ (g = 2.0013) recorded after the chemical oxidation of 3.4×10^{-5} M **1** with 1 equiv. $TAPF_6$ in dry dichloromethane at 293 K.

1$^{\bullet+}$

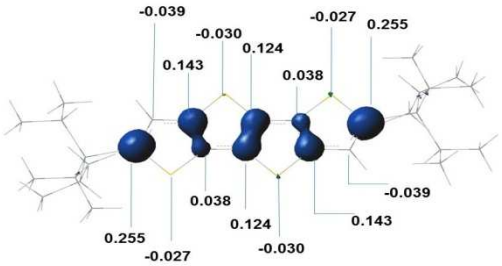

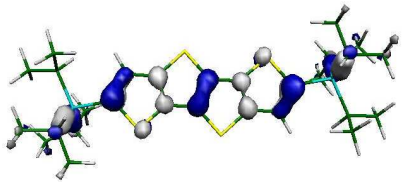

2$^{\bullet+}$

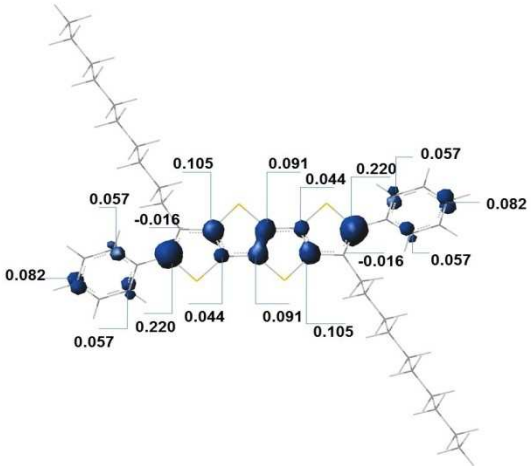

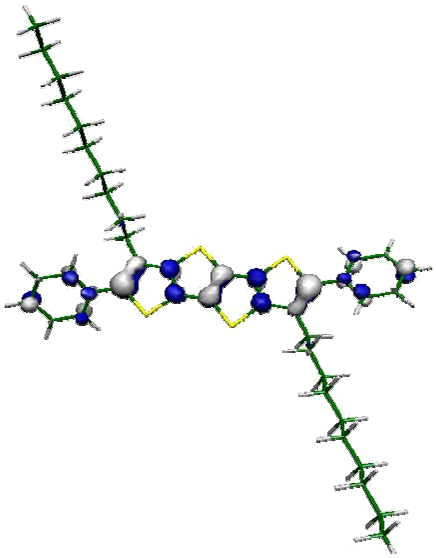

Figure S7 Left: isovalent surfaces (0.004 electron/bohr^3) of spin electron density in the radical cations **1**$^{\bullet+}$ and **2**$^{\bullet+}$ (with n-decyl side chains) calculated at the DFT//M06L/6-31G* level. Mulliken atomic spin densities along the main conjugated CC backbone are also shown. **Right**: SOMO of the radical cations **1**$^{\bullet+}$ and **2**$^{\bullet+}$ calculated at the DFT//M06L/6-31G* level.

3$^{\bullet+}$

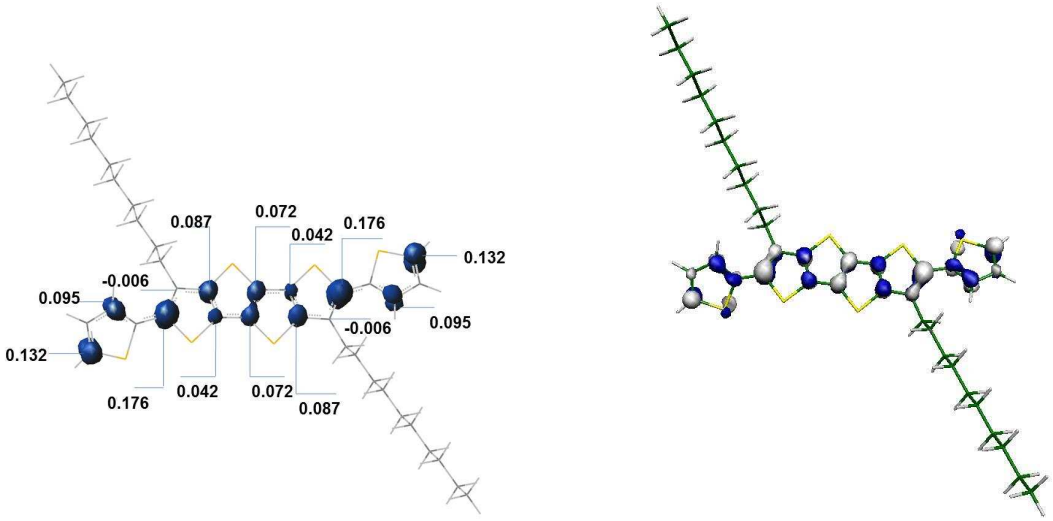

4$^{\bullet+}$

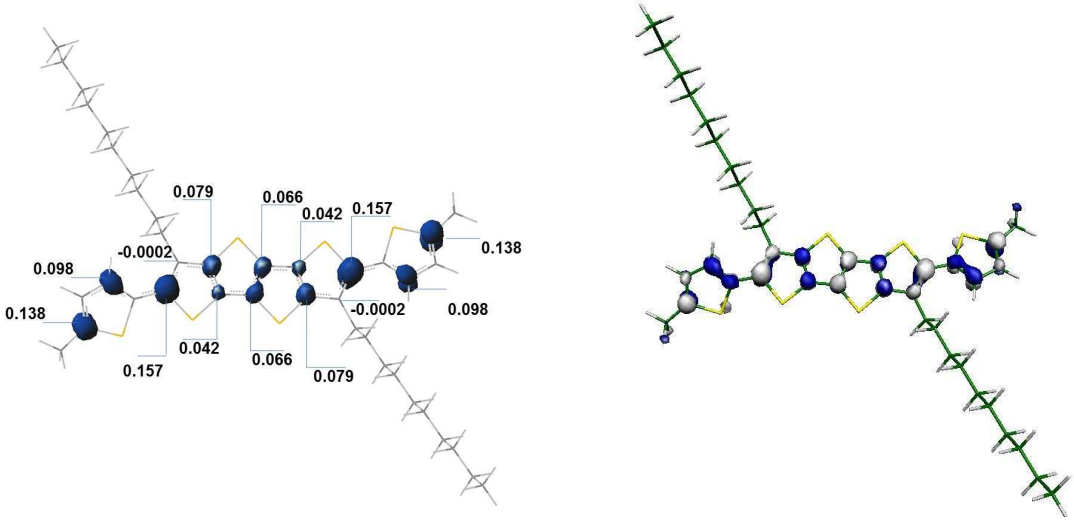

Figure S8 Left: isovalent surfaces (0.004 electron/bohr^3) of spin electron density in the radical cations **3**$^{\bullet+}$ and **4**$^{\bullet+}$ (both with n-decyl side chains) calculated at the DFT//M06L/6-31G* level. Mulliken atomic spin densities along the main conjugated CC backbone are also shown. **Right**: SOMO of the radical cations **3**$^{\bullet+}$ and **4**$^{\bullet+}$ calculated at the DFT//M06L/6-31G* level.

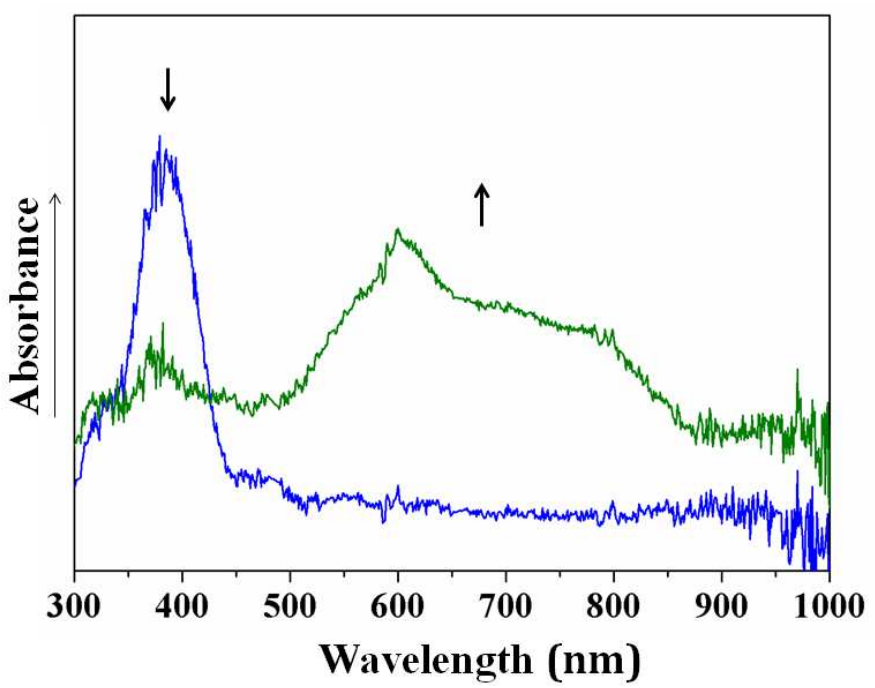

Fig. S9 UV-Vis-NIR spectral changes accompanying the electrochemical oxidation of 5.72×10^{-5} M **3** in $CH_2Cl_2/10^{-3}$ M Bu_4NPF_6 within an OTTLE cell at room temperature. The broad absorption around 800 nm is more intense compared to the spectral changes accompanying the chemical oxidation of **3** to $(\mathbf{3}^{\bullet+})_2$ (see Fig. 4) and continues to grow while keeping the anodic potential of **3** applied. Back reduction by a potentials step to +0.5 V (vs Fc/Fc^+) leads only to a partial recovery of parent **3**; a new species absorbing at 430 nm grows in. Repeated anodic TL-CV scan revealed gradual replacement of the anodic wave of **3** at +0.46 V (vs Fc/Fc^+) with a new one at +0.17 V. This behaviour is tentatively assigned to slow anodic polymerization of the terminal thiophen-2-yl groups, for it was not observed for oxidized **4** bearing the 5-methylthiophen-2-yl substituents. It is consistent with the significant spin density at the pendant thiophen-2-yl rings in $\mathbf{3}^{\bullet+}$ (see Fig. S8).

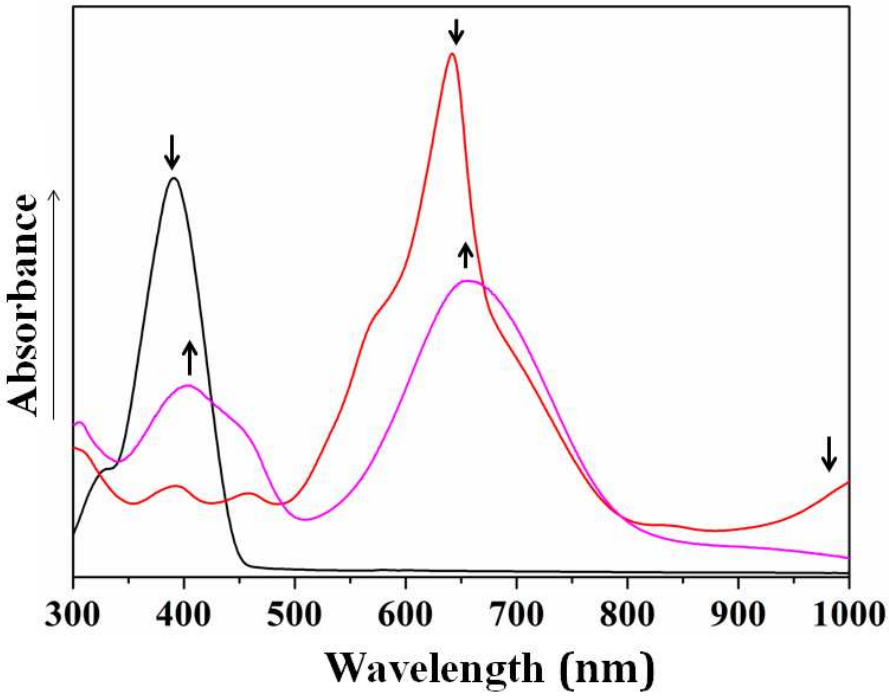

Fig. S10 UV-Vis-NIR spectral changes accompanying the chemical oxidation of 1.80×10^{-4} M **4** with 1 equiv. $TAPF_6$ (red spectrum) and with excess solid $TAPF_6$ (pink spectrum) in dichloromethane containing 0.1 M Bu_4NPF_6 at room temperature.

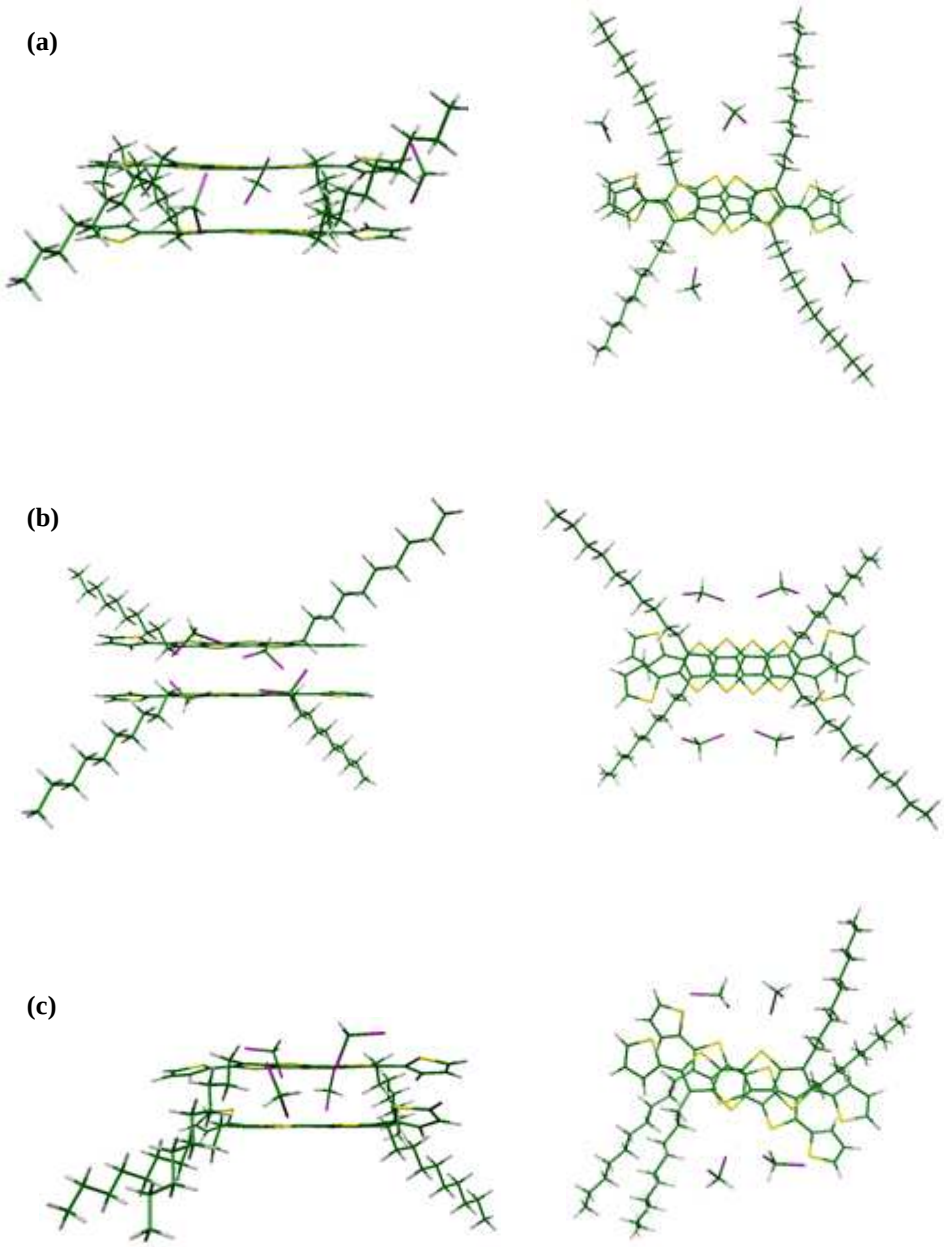

Fig. S11 Lateral (**left**) and top (**right**) views of $(\mathbf{3}^{\bullet+})_2(CH_2Cl_2)_4$ aggregates in their (a) d-d···d-d *anti*- (b) u-u···u-u *anti*- and (c) *syn*-conformations at their optimum M06L/6-31G(d) geometry

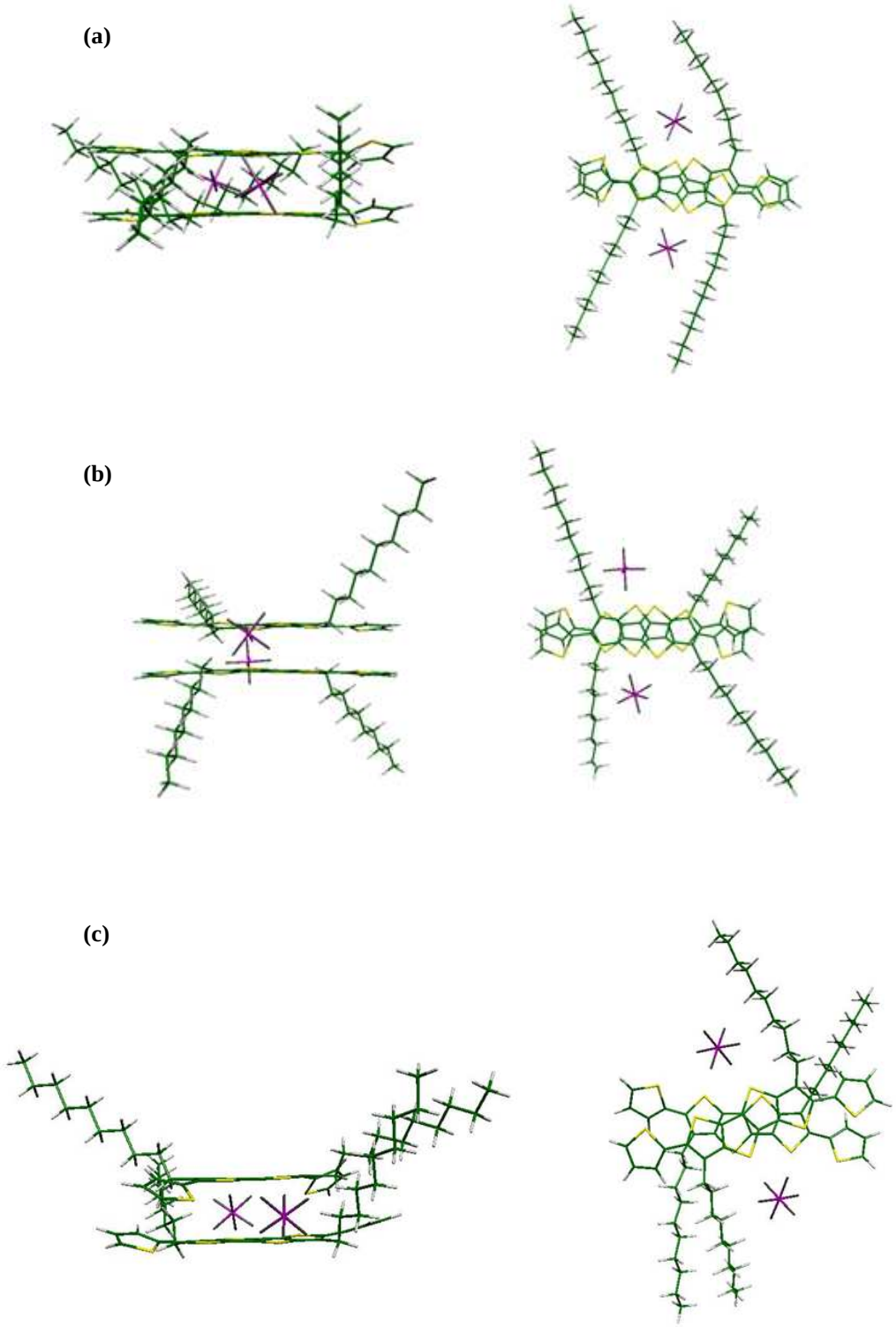

Fig. S12 Lateral (**left**) and top (**right**) views of $(\mathbf{3}^{\bullet+})_2(PF_6^-)_2$ aggregates in their (a) d-d···d-d *anti*- (b) u-u···u-u *anti*- and (c) *syn*-conformations at their optimum M06L/6-31G(d) geometry.

Table S1 Results of TD-DFT calculations of the lowest energy vertical electronic transitions in neutral compounds **1**-**4**. The oscillator strengths *f* (in parentheses) and molar absorption coefficients ε_{max} (dm^3 mol^{-1} cm^{-1}) are also presented. The experimental absorption maxima (λ, in nm) are also shown for comparison.

Compound	λ_{exp} (nm)	ε_{max}	TDDFT//M06L/6-31G(d)		
			λ_{calcd} (nm)	Assignment	HOMO-LUMO gap[b]
1	351 [a]	40 300	355 (1.10)	H→L	2.91 eV
2	360	46 750	415 (1.30)	H→L	2.51 eV
4	385	51 750	446 (1.30)	H→L	2.28 eV
5	391	60 000	456 (1.42)	H→L	2.24 eV

[a] Corresponds to the v′ = 0 vibrational sublevel. [b] Calculated at the DFT//M06L/6-31G(d) level.

Table S2 Lowest energy electronic transitions calculated with TD-DFT// M06L/6-31G(d) for the end-capped tetrathienoacene radical cations at the optimum M06L/6-31G(d) geometries. The calculated oscillator strengths *f* are given in parentheses. The experimental absorption maxima (λ, in nm) are also shown for comparison.

Compound	λ_{exp} (nm)	λ_{calcd} (nm)		Assignment	
1$^{\bullet+}$	740	1079 (0.2)	783 (0.3)[a]	H→S	H-1→S[a]
		440 (0.2)		H-14→S	
	464	433 (0.5)	424 (0.9)[a]	S→L	S→L[a]
2$^{\bullet+}$	935	965 (0.21)		H→S	
	864	863(0.18)		H-2→L	
	519	515 (0.7)		S→L	
3$^{\bullet+}$	993	1005 (0.28)		H→S	
	632	544 (1.23)		S→L	
4$^{\bullet+}$	1216				
	1039	1051 (0.32)		H→S	
	643	564 (1.24)		S→L	
	583				

. [a]Calculated at the TD-DFT//B3LYP/6-31G(d) level for the radical cations at the optimum B3LYP/6-31G(d) geometries.

Table S3 The shortest C···C (inter-chain) distance and interaction energy, E_{int}, of some relevant conformations of $(\mathbf{3}^{\bullet+})_2$ at the optimum M06L/6-31G(d) geometries. The data correspond to the minima on the potential energy curve for the dissociation of the aggregates into two radical cations.

Conformation[a]	***r* (Å)**	**E_{int} (kcal mol^{-1})**
d-d···d-d *anti* $(\mathbf{3}^{\bullet+})_2(CH_2Cl_2)_4$	3.37	-14.8
u-u···u-u *anti* $(\mathbf{3}^{\bullet+})_2(CH_2Cl_2)_4$	3.31	-17.1
syn $(\mathbf{3}^{\bullet+})_2(CH_2Cl_2)_4$	3.39	-15.6
d-d···d-d *anti* $(\mathbf{3}^{\bullet+})_2(PF_6^-)_2$	3.36	-72.8
u-u···u-u *anti* $(\mathbf{3}^{\bullet+})_2(PF_6^-)_2$	3.33	-62.3
syn $(\mathbf{3}^{\bullet+})_2(PF_6^-)_2$	3.39	-72.9

[a] The symbols u (up) and d (down) refer to the mutual orientation of the n-decyl side groups in the models (see Figs S11 and S12).

Table S4 Low energy electronic transitions[a] calculated with TD-DFT for $(\mathbf{3}^{\bullet+})_2(PF_6^-)_2$ and $(\mathbf{3}^{\bullet+})_2(CH_2Cl_2)_4$ aggregates at the optimum M06L/6-31G(d) geometry of the d-d···d-d *anti* conformation, using the M06L and wB97X-D functionals. The calculated oscillator strengths *f* are given in parentheses.

Aggregate	**Electronic transitions**	
TD-DFT//M06L/6-31G(d)		
$(\mathbf{3}^{\bullet+})_2(PF_6^-)_2$	871 nm (0.5) (H-2 → L)	491 nm (1.1) H → L+1
$(\mathbf{3}^{\bullet+})_2(CH_2Cl_2)_4$	919 nm (0.3) (H-2 → L)+ (H-1 → L)	492 nm (1.1) H → L+1
TD-DFT//wB97X-D/6-31G(d)[b]		
$(\mathbf{3}^{\bullet+})_2(PF_6^-)_2$	753 nm (0.9) H-1→ L	407 nm (1.7) (H → L+1)
$(\mathbf{3}^{\bullet+})_2(CH_2Cl_2)_4$	848 nm (1.0) H-1 → L	417 nm (1.7) H-→ L

[a]The experimental electronic absorption spectrum of $(\mathbf{3}^{\bullet+})_2(PF_6)_2$ in CH_2Cl_2 exhibits absorption bands with maxima at 1405 and 642 nm (see Fig.4 in the main text).
[b]wB97XD includes attractive dispersion forces and it was found to give more accurate results for the longer heptathienoacene π–dimer dications[3] than M06L. For the tetrathienoacene compounds, however, similar results are obtained at both M06L and wB97XD levels; this might be ascribed to the shorter length of the tetrathienocene chain that results in a less effective π–π coupling of their backbones in the π-dimer dications.

References

1. Aragó, J.; Viruela, P. M.; Ortí, E.; Osuna, R. M.; Vercelli, B.; Zotti, G.; Hernández, V.; López Navarrete, J. T.; Henssler, J. T.; Matzger, A. J.; Suzuki, Y.; Yamaguchi, S., *Chem. Eur. J.*, **2010**, 16, 5481.

2. Osuna, R. M.; Capel Ferrón, C.; Vercelli, B.; Hernández, V.; Zotti, G.; López Navarrete, J. T., *Portugal. Electrochim. Acta*, **2010**, 28(1), 63.

3. Capel Ferrón, C.; Capdevila Cortada, M.; Balster, R.; Hartl, F.; Niu, W.; He, M.; Novoa, J.J.; López Navarrete, J.T.; Hernández, V.; Ruiz Delgado, M.C. *Paper in preparation.*

Syntheses and preparations

Compounds **1** (ref.[1]) and 2,6-dibromo-3,7-diheptadecanyltetrathienoacene (**Br2-T4**)[2] were prepared according to literature procedures. Their purity was checked by ^{1}H NMR. The syntheses of **2-4** were achieved through either Stille coupling or Suzuki coupling[3] (Scheme 1). The yields vary from 51% to 80% (see below).

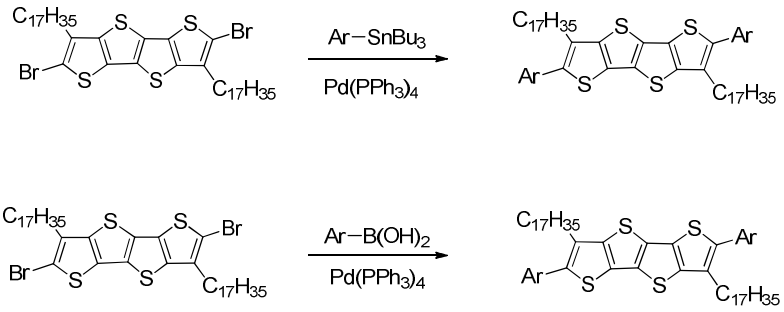

Scheme 1 Synthesis of **2** (Ar = phenyl, top and bottom), **3** (Ar = thiophen-2-yl, top) and **4** (Ar = 5-methylthiophen-2-yl, bottom) through either Stille coupling (top) or Suzuki coupling (bottom).

*Synthesis of **2***

Method 1 (Stille coupling). Compound **Br2-T4** (0.50 g, 0.56 mmol) was placed in a microwave reaction test tube fitted with a stirring bar and phenyl tris(n-butyl)tin (0.52 g, 1.41 mmol) was added. The tube was flushed through by nitrogen for several minutes, then sealed and taken into a glove box. In the glove box, $Pd(PPh_3)_4$ (0.098 g, 0.064 mmol) and toluene (15 mL) were added to the reaction tube. The tube was sealed and seated into a microwave reactor. After 40 min of reaction time at 120 °C in the microwave reactor, the reaction mixture was purified by a silica gel column chromatography (using hot hexane as the eluent). The solvent was removed from the eluent under reduced pressure to yield an oily product to which about 50 mL of methanol / ethanol (1:1 v/v) was added to yield **2** as a light yellowish crystalline solid that was collected by filtration and dried under vacuum (0.25 g, 51% yield). ^{1}H NMR (300 MHz, CD_2Cl_2): δ 7.56-7.36 (m, 10 H), 2.84 (t, J = 7.7 Hz, 4 H), 1.82-1.71 (m, 4

H), 1.47−1.12 (m, 56 H), 0.87 (t, *J* = 6.1 Hz, 6 H). Elemental analysis: calcd: C 76.30; H 9.15; S 14.55, found: C 75.96; H 8.93; S 15.37.

Method 2 (Suzuki coupling). Compound **Br2-T4** (0.29 g, 0.33 mmol) was placed in a microwave reaction test tube fitted with a stirring bar and phenylboronic acid (0.1 g, 0.817 mmol), THF (9 mL) and 20% aqueous sodium carbonate (9 mL) were added. The tube was flushed through by nitrogen for several minutes, then sealed and taken into a glove box. In the glove box $Pd(PPh_3)_4$ (0.113 g, 0.098 mmol) and toluene (3 mL) were added to the reaction tube. The tube was sealed and seated into the microwave reactor. After 40 min of reaction time at 80 °C in the microwave reactor, the organic layer was collected and purified by a silica gel column chromatography (using hot hexane as the eluent). The solvents were removed from the collected eluent under reduced pressure to yield a yellowish solid that was collected by filtration and dried under vacuum (0.23 g, 80% yield). ^{1}H NMR of this yellowish precipitate is the same as that of pure **2** synthesized from Method 1 (Stille coupling).

*Synthesis of **3***

Compound **Br2-T4** (1.64 g, 1.84 mmol) was placed in a microwave reaction test tube fitted with a stirring bar and of thiophen-2-yl tris(n-butyl)tin (1.41 g, 3.78 mmol) was added. The tube was flushed through by nitrogen for several minutes, sealed and taken into a glove box. In the glove box, $Pd(PPh_3)_4$ (0.32 g, 0.28 mmol) and toluene (15 mL) were added to the reaction tube. The tube was sealed and seated into the microwave reactor. After 40 min of reaction time at 120ºC in the microwave reactor, the reaction mixture was purified by a column chromatography (using hot hexane as the eluent). The solvent was removed from the eluent under reduced pressure to yield an oily product to which about 100 mL of methanol / ethanol (1:1, v/v) was added to yield **3** as a yellowish precipitate that was collected by filtration and dried under vacuum (1.31 g, 79% yield). ^{1}H NMR (300 MHz, CD_2Cl_2): δ 7.40 (d, *J* = 5.1 Hz, 2 H), 7.22 (d, *J* = 3.3 Hz, 2 H), 7.12 (br t, *J* = 4.5 Hz, 2 H), 2.93 (t, *J* = 7.8 Hz, 4 H), 1.79 (p, *J* = 7.5 Hz, 4 H), 1.51−1.17 (m, 56 H), 0.87 (t, *J* = 6.6 Hz, 6 H). Elemental analysis: calcd: C 69.90; H 8.57; S 21.53, found: C 69.86; H 8.54; S 21.26.

*Synthesis of **4***

Compound **Br2-T4** (0.41 g, 0.46 mmol) was placed in a microwave reaction test tube fitted with a stirring bar and 5-methylthiophen-2-ylboronic acid (0.16 g, 1.16 mmol), THF (20 mL) and 20% aqueous sodium carbonate (10 mL) were added. The tube was flushed through by nitrogen for several minutes, sealed and taken into a glove box. In the glove box, $Pd(PPh_3)_4$ (0.080 g, 0.069 mmol) was added to the reaction tube. The tube was sealed and seated into the microwave reactor. After 40 min of reaction time at 80 °C in the microwave reactor, the organic layer was collected and purified by a silica gel column chromatography (using hot hexane as the eluent). The solvent was removed from the eluent under reduced pressure to yield a yellowish solid that was recrystallized from hexane to yield pure **4** as a yellowish solid. The solid product was then collected by filtration and dried under vacuum (0.25 g, 59% yield). ^{1}H NMR (300 MHz, CD_2Cl_2): δ 6.99 (d, *J* = 3.4 Hz, 2 H), 6.77 (d, *J* = 3.4 Hz, 2 H), 2.90 (t, *J* = 8.0 Hz, 4 H), 2.53 (s, 6H), 1.77 (quin, *J* = 5.7 Hz, 4 H), 1.49−1.17 (m, 56 H), 0.87 (t, *J* = 6.7 Hz, 6 H). Elemental analysis: calcd: C 70.37; H 8.75; S 20.88, found: C 69.71; H 9.27; S 20.49.

*Equipment used for characterization of **2-4***

Solution ^{1}H NMR spectra were obtained using a Varian UnityInova spectrometer. Microanalyses (C, H, S) were performed on a CE Elantech, Inc. CHNS-O Analyzer, FLASHEA 1112 Series.

Synthesis of thianthrenium hexafluorophosphate ($TAPF_6$)

A modified literature procedure[4] was employed. Thianthrene (2.12 g, 9.80 mmol) and nitrosonium hexafluorophospate, $NOPF_6$ (1.91 g, 10.92 mmol) were placed side by side under argon in a 500 mL round-bottom vessel capped with a septum. Dry butyronitrile (40 mL, distilled from CaH_2) was added into the flask through the septum and argon was bubbled into the solution through a central frit sealed into the vessel close to the bottom, followed by stirring for 2 h. The solution turned green. Then, the vessel was cooled on ice and dry diethyl ether (120 mL) was added in portions. The dark precipitate formed was filtered off, washed with dry diethyl ether and finally dried under vacuum overnight. It was stored under argon. Yield: 1.80 g (4.98 mmol, 51%).

References

1. Okamoto, T.;Kudoh, K.; Wakamiya, A.; Yamaguchi, S. *Chem. Eur. J.*, **2007**, *13*, 548.

2. (a) Matthews, J. R.; Niu, W.; Adama Tandia, A.; Wallace, A.L.; Hu, J.; Lee, W.-Y.; Giri, G.; Mannsfeld, S. C. B.; Xie, Y.; Cai, S.; Fong, H. H.; Bao, Z.; He, M. *Chem. Mater*. **2013**, *25*, 782. (b) Fong, H. H.; Pozdin, V. A.; Amassian, A.; Malliaras, G. G.; Smilgies, D.-M.; He, M.; Gasper, S.; Zhang, F.; Sorensen, M. *J. Am. Chem. Soc.*, **2008**, *130*, 13202.

3. (a) He, M.; Leslie, T. M.; Niu, W. US Patent 7,919,634 April 5, 2011; (b) He, M.; Leslie, T. M.; Niu, W. US Patent 8,278,410 October 2, 2012.

4. Shine, H. J.; Zhao, B.-J.; Marx, J. N.; Ould-Ely, T.; Whitmire, K. H., *J. Org. Chem.*, **2004**, 69, 9255.

.

Spectro-electrochemical techniques, procedures and instrumentation

Preparation of tetrathienoacene solutions for spectro-electrochemistry

The studied end-capped tetrathienoacenes were weighed and dissolved either in an electrolyte solution (typically 10^{-1} M Bu_4NPF_6 in dichloromethane) or in pure dichloromethane, using a Transsonic 470/H stirrer until a homogeneous solution was obtained. Dichloromethane was distilled from CaH_2 under a dry nitrogen gas atmosphere, followed by bubbling with dry argon on a frit for approximately 10 min directly prior to use.

Cyclic voltammetry

Cobaltocenium hexafluorophosphate was used as internal standard[1] for determining electrode potentials and possible effects of adsorption or electrode passivation. The solution was transferred on argon to the air-tight single-compartment electrochemical cell equipped with a Pt microdisk working electrode, a Pt coil counter electrode and a silver wire pseudoreference electrode. The cell was connected to an EG&G PAR Model 283 potentiostat connected to a PC.

Spectroelectrochemistry

The solution was transferred to the optically transparent thin-layer electrochemical (OTTLE) cell[2] with an optical path length of 0.2 mm, equipped with a platinum minigrid working electrode (32 wires per cm) connected to a PA4 potentiostat (Laboratory Devices, Polná, Czech Republic). The parent compound was scanned with a UV-Vis-NIR diode-array spectrophotometer (Scinco S-3100) first and then a positive potential was applied to the working electrode in the thin-layer cell on sweeping from the rest potential at the scan rate of 2 mV s^{-1}. The spectral changes were monitored on passing the anodic wave in the thin-layer cyclic voltammogram at small potential increments.

Single beam UV-Vis-NIR spectroscopy

The solution was transferred to a Schlenk vessel with an attached 2 mm quartz cuvette (Hellma). The sample was scanned rapidly with a UV-Vis-NIR diode-array spectrophotometer (Scinco S-3100) to obtain the electronic absorption spectrum of the parent compound. The $TAPF_6$ oxidant (1 equiv. or in excess) was either added as a solid into the Schlenk vessel under argon or, dissolved in dichloromethane, by titration through a septum. $TAPF_6$ is sparingly soluble in dichloromethane, which allows to oxidize the tetrathienoacene compounds instantly and selectively to radical cations. The remaining non-dissolved solid oxidant is left in the Schlenk vessel. Stepwise addition of an aliquot of a concentrated solution of the oxidant is however preferable. The rapid oxidation with solid $TAPF_6$ is especially convenient in the case of **3** for the EPR spectroscopic study combined with UV-Vis monitoring, where the slowly dimerisation of the radical cations may preclude recording of their well resolved EPR signal.

Double beam UV-Vis-NIR spectroscopy

The samples solutions in 1 mm or 10 mm quartz cuvettes (Hellma) were scanned with a double-beam spectrophotometer (Perkin Elmer Lambda 900) covering the wavelength range down to 3300 nm, to obtain the full NIR spectrum of the oxidized species. Alternatively, a Cary 5000 spectrophotometer was used.

Electron paramagnetic resonance (EPR) spectroscopy

The solution of tetrathienoacene in dichloromethane was oxidized with $TAPF_6$ directly in a narrow EPR tube under an atmosphere of dry argon. Combined EPR and UV-Vis

monitoring experiments were also performed, in particular for compound **4**. The EPR spectra were recorded with a JEOL FR30 X-band EPR spectrometer. Thianthrenium (g_{iso} = 2.0084)[3] and 1,1-diphenyl-2-picrylhydrazyl (g = 2.0036)[4] radicals were used as internal and external standards, respectively.

References

1. Stojanovic, R. S.; Bond, A. M. *Anal. Chem.* **1993**, *65*, 56.

2. Krejčík, M.; Daněk, M.; Hartl, F. *J. Electroanal. Chem*. **1991**, *317*, 179.

3. Giordan, J.; Bock, H. *Chem. Ber*. **1982**, *115*, 2548.

4. Krzystek, J.; Sienkiewicz, A.; Pardi, L.; Brunel, L. C. *J. Magn. Reson.*, **199**, *125*, 207.

Computational details

The molecular geometries of the neutral and radical cationic of compounds **1-4** were calculated at the Density Functional Theory (DFT) level using the M06L[1] and B3LYP[2,3] functionals and the 6-31G* basis[4-6] set, as implemented in the GAUSSIAN09 program.[7] For the geometry optimizations of $(\mathbf{3}^{\bullet+})_2$ π-dimer dication, the M06L functional was chosen due to its ability to describe π–π interactions and estimate the energies of weak intermolecular interactions more efficiently than the B3LYP functional.[8,9] In compounds **2-4**, two n-decyl side chains replaced the two β-heptadecyl side chains in order to reduce the computational cost.

Vertical electronic excitaton energies were computed by using the time-dependent DFT (TD-DFT) approach.[10-12] For the neutral and radical cationic of compounds **1-4**, very similar electronic transitions and trends within the series were obtained when using both M06L and B3LYP functionals. For $(\mathbf{3}^{\bullet+})_2$ π-dimer dication, the vertical electronic excitation energies were calculated using the M06L and wB97XD[13] functionals on the previously optimized M06L/6-31(G) molecular geometries; very similar values are obtained for both methods. Molecular orbital contours were plotted using Molekel 4.3.[14]

References

1. Zhao, Y.; Truhlar, D.G. *J. Chem. Phys.* **2006**, *125*, 194101.
2. Lee, C. T.; Yang, W. T. and Parr, R. G. *Physical Review B* **1988**, *37*, 785-789.
3. Becke, A. D. *Journal of Chemical Physics* **1993**, *98*, 5648-5652.
4. Harihara, P. C.; Pople, J. A. *Theor. Chim. Acta* **1973**, *28*, 213.
5. Hehre, W. J.; Ditchfield, R.; Pople, J. A. *J. Chem. Phys.* **1972**, *56*, 2257.
6. Francl, M. M.; Pietro, W. J.; Hehre, W. J.; Binkley, J. S.; Gordon, M. S.; Defrees, D. J.; Pople, J. A. *J. Chem. Phys.* **1982**, *77*, 3654.
7. Gaussian 09, Revision B.01, M. J. Frisch, G. W. Trucks, H. B. Schlegel, G. E. Scuseria, M. A. Robb, J. R. Cheeseman, G. Scalmani, V. Barone, B. Mennucci, G. A. Petersson, H. Nakatsuji, M. Caricato, X. Li, H. P. Hratchian, A. F. Izmaylov, J. Bloino, G. Zheng, J. L. Sonnenberg, M. Hada, M. Ehara, K. Toyota, R. Fukuda, J. Hasegawa, M. Ishida, T. Nakajima, Y. Honda, O. Kitao, H. Nakai, T. Vreven, J. A. Montgomery, Jr., J. E. Peralta, F. Ogliaro, M. Bearpark, J. J. Heyd, E. Brothers, K. N. Kudin, V. N. Staroverov, T. Keith, R. Kobayashi, J. Normand, K. Raghavachari, A. Rendell, J. C. Burant, S. S. Iyengar, J. Tomasi, M. Cossi, N. Rega, J. M. Millam, M. Klene, J. E. Knox, J. B. Cross, V. Bakken, C. Adamo, J. Jaramillo, R. Gomperts, R. E. Stratmann, O. Yazyev, A. J. Austin, R. Cammi, C. Pomelli, J. W. Ochterski, R. L. Martin, K. Morokuma, V. G. Zakrzewski, G. A. Voth, P. Salvador, J. J. Dannenberg, S. Dapprich, A. D. Daniels, O. Farkas, J. B. Foresman, J. V. Ortiz, J. Cioslowski, and D. J. Fox, Gaussian, Inc., Wallingford CT, 2010.
8. Benitez, D.; Tkatchouk, E.; Yoon, I.; Stoddart, J. F.; Goddard, W. A. J. Am. Chem. Soc. **2008**, *130*, 14928.
9. Capdevila-Cortada, M.; Novoa, J. J. Chemistry – A European Journal **2012**, *18*, 5335.
10. Runge, E.; Gross, E. K. U. Phys. Rev. Lett. **1984**, 52, 997.
11. Gross, E. K. U.; Kohn, W. *Adv. Quantum Chem.* **1990**, *21*, 255.
12. Heinze, H.; Goerling, A.; Roesch, N. *J. Chem. Phys.* **2000**, *113*, 2088.
13. Chai, J.-D.; Head-Gordon, M. *Phys. Chem. Chem. Phys.* **2008**, *10*, 6615.
14. Portmann, S.; Luthi., H. P. *Chimia* **2000**, *54*, 766.